INTERNATIONAL JOURNAL OF ROBUST AND NONLINEAR CONTROL
Int. J. Robust Nonlinear Control 2005; **00**:1–19 *Prepared using* rncauth.cls *[Version: 2002/11/11 v1.00]*

A General Modeling and Control Framework for Electrostatically-Actuated Mechanical Systems

D. H. S. Maithripala[1], B. D. Kawade[1], J. M. Berg[1,*] and W. P. Dayawansa[2]

[1] *Department of Mechanical Engineering, Texas Tech University, sanjeeva.maithripala,b.kawade,jordan.berg@ttu.edu.*
[2] *Department of Mathematics and Statistics, Texas Tech University, daya@math.ttu.edu*

SUMMARY

This paper presents a geometric framework for the stabilization and control of a general class of electrostatically-actuated mechanical systems. Microelectromechanical systems (MEMS), such as micromirrors, are one motivating application for this work. There, wavelengths of applications of interest lead to positioning requirements on the order of forty to one hundred nanometers. Furthermore, electrostatic actuation is poised to be the method of choice for the emerging field of nanoelectromechanical systems (NEMS), and the approach presented should be applicable there as well. The class of devices under study consists of a movable, rigid, grounded electrode, with a variety of allowable rotational and/or translational degrees of freedom, and a set of multiple, fixed, independently-addressable, drive electrodes. A key contribution of this paper places general electrostatic forces in a framework suitable for passivity-based control. The configuration space of the movable body is assumed to have the structure of a simple mechanical system on a Lie group, and stabilizing static and dynamic feedback control laws are derived in terms of coordinate-independent geometric formulas. To obtain controllers for a specific device it is then necessary only to evaluate these formulas. Appropriate approximations may be applied to make the computations more tractable. The static output feedback controller requires only measurement of the charge and voltage on each drive electrode to provide almost-global stabilization of a desired feasible configuration, but performance is limited by the natural dynamics of the mechanical subsystem. Performance may be improved using dynamic output feedback, but additional information is needed, typically in the form of a model relating electrode capacitances to the system configuration. We demonstrate the controller computations on a representative MEMS, and validate performance using ANSYS simulations. Copyright © 2005 John Wiley & Sons, Ltd.

KEY WORDS: Geometric control, MEMS, NEMS, Electrostatic actuation

1. Introduction

Electrostatic actuation of micro- and nanoelectromechanical systems (MEMS and NEMS) makes use of the attractive coulomb forces that develop between capacitively-coupled conductors differing in voltage. Electrostatically-actuated MEMS are popular because they

*Correspondence to: jordan.berg@ttu.edu

Copyright © 2005 John Wiley & Sons, Ltd.

Received XX XXX 2005
Revised 27 May 2005

are simple in structure, flexible in operation, and may be fabricated from standard, well-understood, materials [21]. These same properties make it a good choice for the emerging field of NEMS, such as for the rotational actuator described in [15]. In optical applications, the minimum required device motion is on the order of the smallest wavelength of interest. In fiberoptic applications this is typically 1.3–1.5 μm. For applications such as adaptive optics this may cover the visible spectrum, 400–700 nm. Required precision in positioning will be about one order of magnitude less, that is about 100 nm for communications applications, or about 40 nm for visible light applications. Thus even for MEMS, nanoscale positioning may be required. However, electrostatic actuation is highly nonlinear, making open-loop control over a large operating range difficult. Furthermore, the nonlinearity gives rise to a saddle-node bifurcation called "snap-through" or "pull-in" that results in operational limitations [9, 14, 35, 36, 39, 40, 44, 48]. Bi-stable devices have been designed to exploit the bifurcation [6, 11, 18, 31, 32], however eliminating the effect would allow for enhanced functionality in applications including optical switching [11, 12, 13]; spatial light modulators for image projection [18], data storage, and image recognition [17]; and reconfigurable diffraction gratings for biosensors [52]. When pull-in is the nominal behavior, device lifetimes are often limited by the incremental surface damage done at each contact [31]. Eliminating pull-in would increase the operational range of the movable electrode, reduce the need for motion limiters and anti-stiction measures, and prevent disturbances from causing the movable electrode to depart from its stable operating region.

For the 1-DOF models, several researchers have noted that the bifurcation associated with voltage control disappears when charge is considered as the control input instead of voltage. Charge control has been most directly exploited by Nadal-Guardia, et al., who present open- and closed-loop switching circuits for injecting and maintaining the appropriate amount of charge on the device [33]. This scheme is globally stabilizing but does not address transient behavior. A version of charge control, implemented by means of a switched capacitor circuit is used by Seeger and Boser to stabilize a double-sided 1-DOF electrostatic MEMS [45], and an electrostatic 2-DOF MEMS with both rotational and one dimensional translational degrees of freedom [46]. Lu and Fedder use capacitance measurements to obtain displacement, and apply a classical linear, time-invariant controller design to approximately double the operational range of a parallel plate capacitor [23]. Transients are addressed through an input-shaping pre-filter. These method extends the operational range of the device, but guaranteed stability properties are only local. In [25, 27] we have presented a series of results on global and semi-global stabilization of any point of the gap of an electrostatically actuated 1-DOF devices. These control algorithms can be implemented with static output feedback of the charge on the device and the voltage on the control electrode. Charge can be inferred from capacitance and voltage measurements, where the capacitance measurements are made at a frequency well above the natural frequencies of the device [23]. It can also be obtained by placing an auxiliary electrode in series with the device, and measuring the voltage [3]. This is similar in structure to the capacitive stabilization method [9, 44], but the auxiliary electrode serves only as a sensor, rather than as a combined sensor/actuator. These ideas are extended in [26] to include more complex devices such as membranes and 6-DOF rigid structures. The goal of the present paper is to obtain a control methodology, applicable to a general class of devices, that directly addresses nonlinearity, eliminates pull-in, and allows improvements in transient behavior.

In [25, 26, 27, 28] the electrostatic force due to an actuating electrode is factored as the charge on the electrode squared, times a term possibly depending on the configuration, but

Copyright © 2005 John Wiley & Sons, Ltd.

Prepared using rncauth.cls

independent of voltage or charge. This factorization is used to feedback passify the system and form an appropriate storage function. In those works either this form is justified based on computations specific to the device geometry under study, or it is simply assumed to hold. In Section 2.1 we show that in fact this representation is valid for a general electrode configuration, subject to standard assumptions on the electric field [14, 16, 33, 36]. In this sense, the results presented may be considered to generalize many formulations found in the MEMS and NEMS literature [14, 34, 35, 36, 39, 41, 42, 46, 48]. However use of the model for control will require considerable simplifying assumptions, and so approximation techniques are required. Common approaches include modeling by parallel plate capacitors, following Nathanson [35], and seen in many subsequent works, including [34, 41, 46, 48]. These neglect fringing and other geometry effects. A more accurate approach to approximation is seen in [42] for the special case of circular symmetry. Most works to date, with the notable exception of [34], ignore interelectrode coupling. For example, the work of Nemirovsky and co-workers [14, 36] presents a general framework for computing pull-in parameters for electrostatic systems, but ignores electrode-to-electrode effects. A first-order electrostatic coupling models for multi-electrode systems has recently been presented in [34], which assumes a parallel plate capacitor model for each movable-fixed electrode pair.

In Section 2.2 the general electrostatic force model is integrated into equations of motion for a simple mechanical system with configuration space described by a Lie group. The Lie group setting is quite general, and can incorporate rigid rotation and translation, flexible bodies, and combinations of these.

In Section 3 we present two control laws for such systems. The first requires measurement of the voltage drop from each control electrode to the movable electrode, and the charge on each control electrode. As discussed above, charge can be measured in several ways. This design is effective for stabilization, but not suitable for improving performance, as the natural damping in the mechanical subsystem can shown to be unaffected by the controller. The second design is passivity-based [20, 37, 38] and may be used to inject damping into the mechanical subsystem. Thus, if the transients of the system are under-damped, the second design, which also requires the generalized velocity of the movable electrode, should be used. However it is often the case that the generalized velocity cannot be measured directly. In [24, 27, 28] we propose an observer to provide estimates of the generalized velocity given configuration measurements. Composing this result with the second design yields a dynamic output feedback controller that both stabilizes and improves transient performance. Depending on the properties of the zero dynamics of the system, the controllers may be locally, globally, or almost globally asymptotically stabilizing.

If the system is over-damped, the controller presented cannot be used directly to speed performance. Zhu and co-authors have addressed this concern for 1-DOF electrostatic MEMS by stabilizing pre-computed open-loop trajectories [51]. This approach applied to over-damped systems will outperform the methods presented below. However we note that no such scheme has yet been presented for the general case, and also that it is in principle possible to *reduce* damping, as well as increase it, using passivity-like methods. Thus both approaches remain areas of on-going research interest.

In Section 4 we demonstrate our approach on a representative MEMS device, and validate performance using the finite-element package ANSYS. A highly simplified control model is used for design, but the ANSYS simulation includes electrostatic fringing, non-uniform charge distribution, flexibility of the movable electrode, and geometric nonlinearities. Despite the

Copyright © 2005 John Wiley & Sons, Ltd.

relatively crude control design model, performance is shown to be excellent.

2. Geometric Modeling of an Electrostatically-Actuated Mechanical System

The techniques of geometric mechanics provide a general framework for modeling and control of electromechanical systems. The main advantage of these methods is that they provide a coordinate-free representation of the system dynamics, allowing physical insight and controller design without the notational complexity introduced by choosing coordinates and, if necessary, changing coordinates patches. The controller must ultimately be implemented in coordinates, but this is done only after the design is accomplished.

Results are available when the configuration space in which the electromechanical system evolves is assumed only to be a Riemannian manifold. However, we will consider here the case where the configuration space has the additional structure of a Lie group. The Lie group setting is still quite general, and can incorporate rigid rotation and translation, flexible bodies, and combinations of these.

The approach we will take is to write the Euler-Lagrange equations on the appropriate configuration space in a coordinate-free way. These expressions are the foundation of a general approach to controller design. They may also serve as the basis for open-loop analysis and simulation. The first step is to write the forces acting on the system in a suitable form. This is the subject of the next section, and a main contribution of this paper. We stress that the results provide a general framework for modeling disturbance and control forces—including interelectrode coupling, fringing effects and parasitics—but that the effort needed to obtain explicit expressions in coordinates for a particular geometry may be significant.

2.1. Generalized Electrostatic Forces

In this section we derive an expression for electrostatic forces that is particularly well suited for the geometric framework, and for subsequent controller design. We assume a finite number of perfectly-conducting electrodes. These electrodes may represent movable bodies, fixed control surfaces, and disturbances. The interaction between electrodes is modeled by Laplace's equation in a compact domain with zero potential at the boundary. The result may also be applied to an infinite domain with zero potential at infinity.

The equations of motion arising from these forces are treated in subsequent sections. At that point the choice of configuration space is critical, and is discussed in some detail. However the forces are modeled using a quasi-static approximation, so it suffices for the purposes of this section to denote the instantaneous configuration abstractly by g. This variable may stand, for example, for a rigid rotation matrix, for a function defining the deformation of a flexible body, or for various combinations of these.

For simplicity we detail the calculation only of the electrostatic forces and moments acting on a given electrode. An identical process may be applied to obtain the forces and moments on any electrode of interest. Let the total number of electrodes be $m + 1$, situated inside the domain $\mathcal{U}$, assumed to be a compact subset of $\mathcal{R}^3$. Each electrode is assumed to be a closed subset $\bar{U}_i$ of $\mathcal{U}$, where $i = 0, 1, 2, \cdots, m$. Denote the interior and boundary of $\bar{U}_i$ by $U_i \subset \mathcal{R}^3$ and $\mathcal{S}_i$, respectively. Let $\Omega \subset \mathcal{U}$ be the complement of the set $\cup U_i$ in $\mathcal{U}$, that is, the regions of $\mathcal{U}$ that are not part of any electrode interior. The permittivity in this region is

Copyright © 2005 John Wiley & Sons, Ltd.

assumed constant with value ϵ. Because the electrodes are perfect conductors, they must each be at a constant potential, denoted V_i [16]. In general this will require a net charge, denoted Q_i, on that electrode. For a perfect conductor, Q_i may be found by integrating the surface charge density $\sigma_i(p)$ over $\mathcal{S}_i$ [16]. Applying voltages to some or all the electrodes will induce a potential and an electric field on Ω. We assume that the potential is zero on the external boundary $\tilde{\mathcal{S}} = \partial\Omega / \cup \mathcal{S}_i$. Without loss of generality we assume the force is to be computed on $\bar{U}_0$, and let $Q = [Q_1,\, Q_2,\, \cdots,\, Q_m]^T$ and $V = [V_1,\, V_2,\, \cdots,\, V_m]^T$.

For a given electrode configuration g, let $\phi_i(p, g)$ defined on Ω be the potential at a point $p \in \Omega$ when $V_i = 1$, and all other electrode potentials are zero. (The electrode shapes $\bar{U}_i$, surfaces $\mathcal{S}_i$, and surface normals n_i, are functions of g in general , but this explicit dependence is suppressed for brevity.) Thus $\phi_i(p, g)$ is the unique solution of Laplace's equation $\nabla^2 \phi_i = 0$ subject to the boundary condition $\phi_i|_{\mathcal{S}_j} = \delta_{ij}$, where δ_{ij} is the Kronecker delta. Uniqueness and linearity of solutions imply that $\phi(p, g, V_0, V) = \sum_{i=0}^{m} V_i\, \phi_i(p, g)$ is the unique solution corresponding to the boundary condition $\phi|_{\tilde{\mathcal{S}}} = 0$ and $\phi|_{\mathcal{S}_i} = V_i$, $i = 0, \cdots, m$. Then the electrostatic field intensity at a point p in space is given by

$$E(p, g, V_0, V) = \nabla\phi(p, g, V_0, V) = \sum_{i=0}^{m} V_i\, \nabla\phi_i(p, g).$$

The electrostatic field is always perpendicular to the electrodes and the electrostatic field inside a conductor is zero. Hence application of Gauss' law yields that the magnitude of the electrostatic field at the surface $\mathcal{S}_i$ is $\sigma_i(p)/\epsilon$ [16], where $\sigma_i(p)$ is the surface charge density at a point p on $\mathcal{S}_i$. Thus the charge density must be

$$\sigma_i(p, g, V_0, V) = \sum_{j=0}^{m} \epsilon V_j\, \nabla\phi_j(p, g) \cdot n_i(p),$$

where $n_i(p)$ is the unit outward pointing normal at p to $\mathcal{S}_i$. Thus the total charge on $\bar{U}_i$ is

$$Q_i = \sum_{j=0}^{m} \epsilon V_j \int_{\mathcal{S}_i} \nabla\phi_j(p, g) \cdot n_i(p)\, ds. \tag{1}$$

Define the general capacitances

$$C_{ij}(g) = \int_{\mathcal{S}_i} \epsilon \nabla\phi_j(p, g) \cdot n_i(p)\, ds.$$

Then $Q_i = \sum_{j=0}^{r} C_{ij}(g) V_j$. To make subsequent calculations more compact, we now specialize the equations to the situation of interest for later sections, in which only $\bar{U}_0$ can move, and $V_0 = 0$. Then in matrix notation $Q = C(g)V$ where $C(g) = [C_{ij}(g)]$, $i, j = 1, \cdots, m$. It can be easily verified that the mapping $C(g) : \mathcal{R}^m \mapsto \mathcal{R}^r$ is one-to-one and onto and so a unique $C^{-1}(g) = [C^{ij}(g)]$ exists. Then also $V = C^{-1}(g)Q$.

The electrostatic force acting on a unit charge at the surface of a conducting electrode is $E/2$ [16]. Thus the force δf^e acting at a point p on $\mathcal{S}_0$ is

$$\delta f^e = \frac{1}{2} \sum_{i=1}^{m} \epsilon V_i \left(\sum_{j=1}^{m} V_j (\nabla\phi_j \cdot n)(\nabla\phi_i \cdot n) \right) n, \tag{2}$$

Copyright © 2005 John Wiley & Sons, Ltd.

where n is the unit outward normal to $\mathcal{S}_0$ at the point p. Defining the matrix $\tilde{f}(p,g) = [\tilde{f}_{ij}(p,g)]$ as

$$\tilde{f}_{ij}(p,g) = \epsilon(\nabla\phi_j \cdot n)(\nabla\phi_i \cdot n)$$

we have that

$$\delta f^e = \frac{1}{2}\sum_{i=1}^{m}\sum_{j=1}^{m}\Big(V_i\,\tilde{f}_{ij}(p,g)\,V_j\Big)\;n(p) = \frac{1}{2}V^T\tilde{f}(p,g)V\;n(p)$$

Observe that the matrix $\tilde{f}(p,g)$ is symmetric.

Noting that $V = C^{-1}Q$ we can also express $\delta f^e(p,g)$ as,

$$\delta f^e = \frac{1}{2}Q^T f(p,g)Q, \tag{3}$$

where $f(p,g) = {C^{-1}}^T\tilde{f}(p,g)C^{-1}$ is again symmetric.

This last expression is the major contribution of this section, because it shows that the magnitude of the electrostatic forces is a quadratic form of the electrode charges, Q. This will prove to be critical in applying control techniques for feedback passifiable systems [8]. We also emphasize that this model takes into consideration fringing, parasitics, and interelectrode coupling. Fringing is included in the $\phi_i(p,g)$, which are complete solutions to the electrostatic equations. Parasitics may be incorporated as uncontrolled electrodes. Interelectrode coupling enters as the off-diagonal terms of the capacitance matrix $C(g)$, and in the off-diagonal terms of $\tilde{f}(p,g)$ and $f(p,g)$. In this sense, the above formulation may be considered to generalize many formulations found in the MEMS and NEMS literature, such as [14, 34, 35, 36, 39, 41, 42, 48, 46] However explicit computation of these terms requires solution of Laplace's equation at each possible configuration g. This is rarely practical without considerable simplifying assumptions, and so approximation techniques, as explored in the references, will continue to be a research focus.

Common approaches include modeling by parallel plate capacitors, following Nathanson [35], and seen in many subsequent works, including [34, 41, 46, 48]. These neglect fringing and other geometry effects. A more accurate approach to approximation is seen in [42] for the special case of circular symmetry. Most works to date, with the notable exception of [34], ignore interelectrode coupling. For example, the work of Nemirovsky and co-workers [14, 36] presents a general framework for computing pull-in parameters for electrostatic systems, but ignores electrode-to-electrode effects. A first-order electrostatic coupling models for multi-electrode systems has recently been presented in [34], which assumes a parallel plate capacitor model for each movable-fixed electrode pair.

Finally, we have assumed here that the electrostatic forces are given by Laplace's equation. While true NEMS may require a different model, incorporating electrodynamics and quantum effects, to our knowledge this is not the case for the present generation of devices.

2.2. Generalized Electrostatically-Actuated MEMS Model

We now incorporate the force model derived above into a dynamical model for a general electrostatically-actuated device. The model consists of a mechanical subsystem, coupled through electrostatic forces to an electrical subsystem. For convenience we assume that only $\bar{U}_0$ is free to move, that the other electrodes are fixed in space, and that $V_0 = 0$. The problem of configuration control of a single movable electrode using multiple actuators has many practical

Copyright © 2005 John Wiley & Sons, Ltd.

device applications, and is considered, for example, in [36]. Extension to the more general case of multiple moving electrodes with assignable potentials is straightforward. The configuration of the mechanical system is denoted by g, which is an element of the configuration space G. The mechanical system is assumed to satisfy the Euler-Lagrange equations with generalized forcing (the Lagrange-d'Alembert equations), where the forces are due to conservative mechanical terms, Rayleigh damping, and the electrostatic coupling derived in the previous section. In principle G can be finite- or infinite-dimensional [30]. For a detailed consideration of infinite-dimensional devices such as flexible beams, plates, and membranes see, for example, [41]. The remainder of this paper will assume rigid-body motion, and hence focus on the finite-dimensional case.

Each fixed electrode $\bar{U}_i$ is assumed to be a capacitive element within a circuit also consisting of a voltage source u_i and series resistor r_i. Define matrix $R = diag(r_1, r_2 \cdots, r_m)$ and vector $U = [u_1, u_2, \cdots, u_m]^T$. The loop currents are denoted J_i, with $J_i = \dot{Q}_i$, and

$$r_i \dot{Q}_i = u_i - V_i \,. \tag{4}$$

Electrodes are designated as either control electrodes when the source voltage can be arbitrarily assigned, or disturbance electrodes when it cannot.

Using (3) we derive the resultant electrostatic force and torque on the movable rigid electrode. The configuration space for general rigid body motion is the Lie group $SE(3)$. Constrained motions can be obtained from the expressions for $SE(3)$, and multiple rigid movable electrodes may be treated as the product of these cases. Some specific examples are presented in later sections.

Let $\{e_1, e_2, e_3\}$ be a body fixed coordinate system fixed at the center of mass of the movable electrode. In these coordinates $n(p) = \alpha_i(p, g) e_i$ and

$$\delta f^e(p) = \frac{1}{2} \sum_{k=1}^{3} V^T \tilde{f}_k(p, g) V \; e_k, \tag{5}$$

where $\tilde{f}_k(p, g) = [\alpha_k(p, g) \tilde{f}_{ij}(p, g)]$ is symmetric. Then the total resultant force acting on the moving electrode takes the form

$$f^e = \frac{1}{2} \sum_{k=1}^{3} V^T \tilde{f}^e_k(g) V \, e_k, \tag{6}$$

with $\tilde{f}^e_k(g) = \int_{\mathcal{S}_0} \tilde{f}_k(p, g) \, ds$ symmetric. Similarly it can be shown that the total resultant electrostatic moment about the center of mass of the moving electrode is given by

$$T^e = \frac{1}{2} \sum_{k=1}^{3} V^T \tilde{T}^e_k(g) V \, e_k, \tag{7}$$

with $\tilde{T}^e_k(g)$ symmetric. Noting that $V = C^{-1} Q$ we can express the resultant electrostatic force f^e and the resultant electrostatic torque T^e, also as

$$f^e = \frac{1}{2} \sum_{k=1}^{3} Q^T f^e_k(g) Q \, e_k, \tag{8}$$

Copyright © 2005 John Wiley & Sons, Ltd.

where $f_k^e(g) = {C^{-1}}^T \tilde{f}_k^e(g) C^{-1}$ is symmetric, and

$$T^e = \frac{1}{2}\sum_{k=1}^{3} Q^T T_k^e(g) Q\, e_k, \tag{9}$$

where $T_k^e(g) = {C^{-1}}^T \tilde{T}_k^e(g) C^{-1}$ is symmetric.

Using these forces combined with the potential and Rayleigh type damping forces acting on the system, the equations of motion for a rigid electrode free to move in three dimensional space can written down using the Lagrange-d'Alembert's principle. The configuration space of the mechanical system is the group of rigid body rotations and translations, $SE(3) \simeq SO(3) \times \mathcal{R}^3$. At a given time the configuration g of the movable electrode is described by the pair $(R, b) \in SO(3) \times \mathcal{R}^3$. Then the equations of motion are given by

$$\begin{bmatrix} \dot{R} & \dot{b} \\ 0 & 0 \end{bmatrix} = \begin{bmatrix} R & b \\ 0 & 1 \end{bmatrix}\begin{bmatrix} \hat{\Omega} & v \\ 0 & 0 \end{bmatrix} \tag{10}$$

$$\begin{bmatrix} \dot{\Omega} \\ \dot{v} \end{bmatrix} = I^{-1}\left(\begin{bmatrix} I_b\Omega \times \Omega \\ Mv \times \Omega \end{bmatrix} + f^c(R,b) + f^d(R,b,\Omega,v) + F^e(Q,R,b)\right), \tag{11}$$

where $f^c(R,b)$ and $f^d(R,b,v,\Omega)$ are the conservative and rayleigh type damping forces, respectively. The generalized electrostatic force $F^e(Q,R,b)$ is given by $F^e = [T^e \quad f^e]^T$, where f^e and T^e are given by (8) and (9) respectively. The inertia tensor of the rigid body is I_b and mass of the rigid body is M. The term $\hat{\Omega}$ is the skew symmetrized version of the vector $\Omega \in \mathcal{R}^3$. For additional details we refer the reader to [28] and the references there in.

We now generalize these ideas to the case where the configuration space of the movable electrode is a finite dimensional Lie group and its dynamics satisfy the forced Euler-Lagrange (Lagrange-d'Alembert) equations. The following mathematical notations and preliminaries will be needed in the description of the model. Let the configuration variable and body velocities of the mechanical subsystem be denoted by $g(t)$ and $\zeta(t)$, respectively. Mathematically $g(t)$ is an element of a Lie group G and ζ is an element of the Lie algebra of the Lie group, $\mathcal{G} \simeq T_eG$ [1, 30]. The left translation of $\zeta \in \mathcal{G}$ to T_gG will be denoted by $g \cdot \zeta = DL_g\,\zeta$. The Lie bracket on $\mathcal{G}$ for any two $\zeta, \eta \in \mathcal{G}$ will be denoted by $[\zeta, \eta] = ad_\zeta\,\eta$ and the dual of the ad operator will be denoted by ad^*. Let $\{e_i\}$ be any basis for the Lie algebra $\mathcal{G}$ and let $\{\sigma^i\}$ be the dual left-invariant one form basis for the dual of the Lie algebra, $\mathcal{G}^*$. Let $I(g) : \mathcal{G} \mapsto \mathcal{G}^*$, for each $g \in G$, be an isomorphism such that the relation $\langle\langle \zeta\,,\,\eta \rangle\rangle_{\mathcal{G}} = \langle I(g)\zeta\,,\,\eta\rangle$ for $\zeta, \eta \in \mathcal{G}$ defines an inner product on $\mathcal{G}$. Here $\langle\cdot,\cdot\rangle$ denotes the usual pairing between a vector and a co-vector. Identifying $\mathcal{G}^*$ and $\mathcal{G}$ with $\mathcal{R}^n$, let $I_{ij}(g)$ and $I^{ij}(g)$ be the matrix representation of $I(g)$ and $I^{-1}(g)$ respectively. Note that $I(g)$ is symmetric and positive definite. If $I(g)$ is smooth in g then such an $I(g)$ induces a unique metric on G by the relation $\langle\langle g\cdot\zeta\,,\,g\cdot\eta\rangle\rangle = \langle I(g)\zeta\,,\,\eta\rangle$ and further it also follows that every metric has such an associated family of isomorphisms. If the metric is Left invariant then I is a constant and any constant symmetric positive definite matrix induces a Left invariant metric on G. We assume that the kinetic energy of the mechanical system is given by this metric [1, 30]. That is the kinetic energy is assumed to be $\frac{1}{2}\langle I\zeta, \zeta\rangle = I\zeta \cdot \zeta$. For rigid body motions I represents the inertia tensor of the rigid body.

The potential energy of the mechanical subsystem is $U_c(g)$. Let $f^c(g)$ be the resultant conservative forces acting on the movable electrode while $f^d(g,\zeta)$ denote Rayleigh-type

Copyright © 2005 John Wiley & Sons, Ltd.

dissipative forces acting on the movable electrode. The model is now given by

$$\dot{Q} = -\Lambda^{-1}(V - u), \tag{12}$$

$$\dot{g} = g \cdot \zeta, \tag{13}$$

$$\dot{\zeta} = I^{-1}\left(ad^*_\zeta I\zeta + f^c(g) + f^d(g,\zeta) + \sum_{k=1}^{n} \frac{1}{2} Q^T f^e_k(g) Q \,\sigma^k\right), \tag{14}$$

where $(g,\zeta) \in TG \simeq G \times \mathcal{G}$ and $\Lambda = diag(r_1, r_2, \cdots, r_r)$. Equation (12) describes the electrical part of the system. In general V should be replaced by $C(g)^{-1}Q$ to make these state equations, however we will later assume that the electrode voltages are available for measurement. In that case the form shown above will be more convenient. Equation (13) describes the kinematics, while (14) is the Euler-Lagrange equation with external forcing for a general rigid body. The $f^e_k(g)$ are now the *generalized* electrostatic forces, which in the specific case of $SE(3)$ derived above would include the moments $T^e_k(g)$ as well. The index n is the dimension of G. The term $ad^*_\zeta I\zeta$ describes the forces that arise from the non-Euclidean nature of G. These are variously known as inertial or apparent forces and include, for example, coriolis terms. Further details on modeling of simple mechanical systems in an intrinsic geometric framework can be found in the excellent texts of [1, 5, 7, 30]. The Appendix contains a concise description of the necessary geometric notations and ideas.

Examples of rigid models specializing (12)–(14) are 1-DOF piston motion, in which $G = \mathcal{R}$, tilting ($G = SO(2) \simeq S$), combined tilting and piston mode ($G = SO(2) \times \mathcal{R} \simeq S \times \mathcal{R}$), in-plane translation and rotation ($G = SE(2)$), 3-DOF rotation about a fixed point ($G = SO(3)$), and unconstrained 3-D translation and rotation ($SE(3)$).

3. Static and Dynamic Output Feedback Stabilization

In this section we show how the general model formulated above may be incorporated into a feedback control design for stabilization and performance enhancement. To focus the discussion on the suitability of (12)–(14) for this purpose, we make additional simplifying assumptions on the electrical components and the available measurements. First, we neglect parasitic effects. That is, all m electrodes are control electrodes, with all u_i available for direct manipulation. Next, as mentioned above, we assume all electrode voltages are available for measurement. Finally, we assume that the charge on each electrode is known. This last may be accomplished in several ways. The current in each control circuit may be monitored, or the electrode charges induced directly, as in [33]. The voltage of auxiliary electrodes may be measured, as in [3]. The capacitance across the drive electrodes may be measured with a high frequency probe signal, and Q then found from $Q = CV$. Finally, the configuration may be measured directly, and Q inferred from a capacitance model and the electrode voltage measurement. Direct measurement of g is typically impractical, except for laboratory demonstration projects. However if Q is measured or found by other means, g may be estimated from the measured V by inverting a model for $C(g)$ [3].

Passivity methods require that system inputs and outputs be specified. The natural inputs are the control voltages u. We will henceforth set the output to be the deviation of the electrode charges Q from some setpoint values $\bar{Q}$, $y = h(Q) \equiv Q - \bar{Q}$. With respect to this output the zero

Copyright © 2005 John Wiley & Sons, Ltd.

dynamics of the system (12)–(14) correspond exactly to the mechanical subsystem (13)–(14) with $Q \equiv \bar{Q}$ [27, 28].

An equilibrium point is said to be locally (respectively, almost globally, globally) asymptotically stable if it is locally stable, and if all trajectories that originate from a neighborhood of the equilibrium (respectively, an open and dense subset of the state space, the entire state space) converge to that equilibrium. We provide two control laws and show that they are locally (respectively, almost globally, globally) asymptotically stabilizing, when the system is locally (respectively, almost globally, globally) *weakly minimum phase* with respect to y, and an additional detectability condition is satisfied. This detectability condition is that whenever the output converges to zero asymptotically, the state must also converge asymptotically [8].

The notion of minimum phase employed in this paper corresponds to that of [8]. Specifically, with respect to the output y, the system (12)–(14) is said to be *locally weakly minimum phase* if the following three conditions are satisfied: i), the equilibrium $(\bar{g}, 0)$ of the system (13)–(14) is locally stable with $Q \equiv \bar{Q}$; ii) there exists a smooth positive definite function $U(g)$ with a local non-degenerate minimum at $\bar{g}$, and iii) the derivative of $W_c = U(g) + 1/2\, I\zeta \cdot \zeta$ along the forced dynamics of the system is negative semi-definite (i. e. $\dot{W}_c = \frac{1}{2}\sum_{k=1}^{n} \zeta^k \bar{Q}^T f_k^e \bar{Q} + \langle f^d, \zeta\rangle + \langle f^c, \zeta\rangle + \langle dU, g\zeta\rangle \le 0$). Without loss of generality we set $U(\bar{g}) = 0$. The function $U(g)$ is the potential energy of the *controlled* mechanical subsystem obtained by *shaping* the potential energy $U_c(g)$ of the unforced mechanical system using the electrostatic forces $Q^T f_k^e Q\, \sigma^k/2$, so that the corresponding controlled equilibrium $(\bar{g}, 0)$ is locally stable. (The quantity W_c is the total energy of the controlled mechanical system, obtained by adding the mechanical kinetic energy to $U(g)$.) For a given $\bar{Q}$ the feasible equilibria are given by $U^{-1}(0)$. If such a $U(g)$ exists we can stabilize any feasible configuration by charge feedback control. The existence of a suitable $U(g)$ depends on the number of independently-addressable electrodes and the form of $f_k^e(g)$. A *necessary* condition is that $df^e(g) \equiv 0$.

The system is said to be *almost globally* weakly minimum phase if it is locally weakly minimum phase, $\bar{g}$ is the unique minimum of $U(g)$ and $U(g)$ is proper. The system is said to be *globally* weakly minimum phase if $\bar{g}$ is the *only* critical point of $U(g)$. For the case $G = \mathcal{R}$ it can be shown that the system (12)–(14) is globally weakly minimum phase [27]. For other problems this property must be investigated on a case-by-case basis.

When the detectability condition is not satisfied asymptotic stability cannot be guaranteed. For detectability to hold it is sufficient to show that the zero dynamics are (locally, almost globally, or globally) asymptotically stable, in addition to being (locally, almost globally, or globally) weakly minimum phase. This has been proven when $G = \mathcal{R}$ [27]. More generally detectability must be verified, as discussed further below.

3.1. Static Output Feedback

Under the assumptions made above, the system (12)–(14) can be stabilized using *static output feedback*, with the region of convergence dependent on the properties of the zero dynamics—in this case exactly the mechanical subsystem with the charge fixed at its equilibrium value. In this case the mechanical subsystem will keep its open-loop dynamics, and thus highly under- or over-damped systems will demonstrate bad transient performance.

Because static output feedback is limited in its ability to affect performance, we present it very briefly. Also analysis of the general case is easily extended from $G = \mathcal{R}$, which is discussed

Copyright © 2005 John Wiley & Sons, Ltd.

in [27, 28].

With measurements of V and Q we implement the static output feedback law

$$u = V - k(Q - \bar{Q}), \tag{15}$$

This control input/output linearizes the system (12)–(14) with respect to the output $h(Q) = Q - \bar{Q}$. The linearized portion is the electrical subsystem (12), and its unique equilibrium point $\bar{Q}$ is now globally exponentially stable with poles $-k\Lambda^{-1}$. The equations are in zero dynamic canonical form [19], and the zero dynamics are exactly (13)–(14) with $Q \equiv \bar{Q}$. As discussed above, asymptotic convergence of the zero dynamics is sufficient for asymptotic stability of the closed loop system. It can be shown by a straightforward but somewhat technical extension of [27] that for the system (12)–(14) and the control (15), this condition is also necessary.

The control (15) is completely independent of mechanical system characteristics such as the inertia tensor, and the damping, potential, and electrostatic forces. Thus the implementation of (15) does not require knowledge of these quantities. This implies that (15) robustly stabilizes the system for all parameter variations that do not destroy the weak minimum phase property of the system. However the convergent equilibrium configuration $U^{-1}(0)$ of the movable electrode $\bar{g}$ explicitly depends on $\bar{Q}$. Thus the exact stable equilibrium configuration depends on the system parameters. Since $\bar{g}$ is a non-degenerate minimum of $U(g)$, for small parameter variations the equilibrium configuration will remain close to $\bar{g}$. To accommodate larger disturbances or parameter variations, the above framework could be used to obtain an adaptive controller.

An inherent drawback of the static feedback scheme is that damping cannot be added to the dynamics of the mechanical subsystem, which constitute the zero dynamics of the closed-loop system. This can be seen from the *necessity* of the asymptotic stability of the zero dynamics. Thus an underdamped mechanical subsystem will cause the performance of the device to suffer from long settling times and large overshoots. It is known that in order to inject significant damping into a mechanical system, velocity feedback is necessary. The next section revisits this principle from a passivity perspective.

3.2. Dynamic Output Feedback

In the previous section it was seen how to stabilize a feasible configuration of the movable electrode, subject to the appropriate weakly minimum phase condition. This result generalizes many results on charge feedback that may be found in the MEMS literature [9, 33, 44, 45, 46]. However, as shown above, no pure charge feedback scheme such as these is capable of altering the transient behavior of the mechanical subsystem. This section shows how the transient behavior may be improved by using passivity ideas in a general geometric framework—the second major contribution of this paper.

If with the output $h(Q) = Q - \bar{Q}$ the system (12)–(14) is locally weakly minimum phase then we will show that with $K > 0$ a positive definite symmetric matrix the control

$$u = V - \frac{1}{2}\sum_{k=1}^{n} \zeta^k \Lambda f_k^e(g)(Q + \bar{Q}) - \Lambda K(Q - \bar{Q}). \tag{16}$$

locally stabilizes the equilibrium $(\bar{Q}, \bar{g}, 0)$. Convergence is asymptotic if the system is detectable to $(\bar{Q}, \bar{g}, 0)$. Once again, the result is global or almost global if the zero dynamics have the corresponding weakly minimum phase properties.

Copyright © 2005 John Wiley & Sons, Ltd.

We first input/output linearize (12)–(14) by setting $u = V + \nu$ and consider the candidate storage function

$$W(Q, g, \zeta) = \frac{1}{2}(Q - \bar{Q})^T (Q - \bar{Q}) + W_c. \tag{17}$$

Taking the derivative of W along the input/output linearized system, and using the symmetry of $f_k^e(g)$ to show that

$$f^e = \frac{1}{2}\sum_{k=1}^{n} Q^T f_k^e Q = \frac{1}{2}\sum_{k=1}^{n} \left(\bar{Q}^T f_k^e \bar{Q} + (Q - \bar{Q})^T f_k^e (Q + \bar{Q}),\right)$$

we have

$$\dot{W} = (Q - \bar{Q})\Lambda^{-1}\nu + \frac{1}{2}\sum_{k=1}^{n} \zeta^k (Q - \bar{Q})^T f_k^e (Q + \bar{Q}) + \dot{W}_c.$$

Thus setting $\nu = -\frac{1}{2}\sum_{k=1}^{n} \zeta^k \Lambda f_k^e(g)(Q + \bar{Q}) - \Lambda K(Q - \bar{Q})$, $\dot{W} \leq 0$ holds locally if the zero-dynamics are weakly minimum phase. Therefore (16) locally stabilizes the equilibrium $(\bar{Q}, \bar{g}, 0)$. Detectability is satisfied here if $Q \equiv \bar{Q}$ implies $\zeta = 0$ and $g = \bar{g}$. This may be checked for any electrode geometry from the rank of the map $[f_1^e(g)\bar{Q} \;\; f_2^e(g)\bar{Q} \;\; \cdots \;\; f_n^e(g)\bar{Q}]$. Full column rank of this matrix implies detectability. A necessary condition for this is that the number of electrodes, m, be equal to the dimension, n, of the configuration space. With detectability, local asymptotic stability of the closed-loop system follows, and the result holds almost globally or globally if the zero-dynamics have the corresponding minimum phase properties. In the static output feedback case we showed that asymptotic stability of the zero dynamics was necessary and sufficient for detectability. the rank condition cited here does not imply asymptotic stability of the zero dynamics, and so this condition is in general only sufficient. This has been explicitly shown for the case $G = \mathcal{R}$ [27]. Thus even devices with undamped mechanical subsystems may be asymptotically stabilized using velocity feedback, if the control electrodes are appropriately positioned. It can also be shown that this is true for the case $G = \mathcal{R} \times SO(2)$ treated in section 4.

Feedback law (16) contains the electrostatic forces, the voltage and charge on the drive electrodes, and the velocity of the movable electrode. Of these, we have assumed only the drive electrode voltage and charge to be measureable. In the examples given below, we use a model for the electrostatic forces. Generally this will be as a function of configuration, which may be estimated using a capacitance model as discussed above. However, we will see that even very simple models seem to result in good performance. Such robustness is often claimed as a benefit of the passivity framework [20, 37, 38]. Velocity assumed not to be measureable, but may be estimated using a dynamic observer and a position estimate based on a capacitance model [24, 27, 28]. The observer, in conjunction with (16), is therefore a dynamic output feedback controller. Using results proven by the authors in [29] it can be shown that if the initial observer error is sufficiently small, the closed-loop system under dynamic output feedback retains the convergence properties of the full-state feedback (16).

4. Example: 2-DOF Tilting and Piston Mode Actuators

In this section we demonstrate our approach on a MEMS mirror modeled as a movable rigid top plate with mass m and moment of inertia about the center of mass I. The electrode model has

Copyright © 2005 John Wiley & Sons, Ltd.

Prepared using rncauth.cls

one translational and one rotational degree of freedom, each associated with a linear spring. The vertical displacement is denoted x and measured from the zero voltage equilibrium position, with the upward direction positive. The rotation θ is about the out-of-plane axis, with anti-clockwise rotation positive. The configuration space of this is $G = \mathcal{R} \times SO(2)$. Two control electrodes of identical length l and areas A are fixed below the movable electrode.

The implementation of the control (16) requires a model of the electrostaic forces. The explicit computation of these require that we solve the Laplace's equation under very general conditions. This may not be possible without additional simplifying assumptions. Even if fringing, inter-electrode coupling and parasitics are neglected the resulting electrostatic force model may still be complicated. For instance, under these assumptions the self capacitance, C_{11}, of the first electrode f^e_{11} appearing in the the electrostatic force quadratic term takes the form

$$C_{11} = \frac{\epsilon A}{l\theta} \ln\left(\frac{d-x}{d-x-l\sin\theta}\right), \quad f^e_{11} = -\frac{\epsilon A \tan^2\theta\cos\theta}{C_{11}^2\theta^2(d-x)(d-x-l\sin\theta)},$$

respectively. Even though these expressions can be used in the controller design we deliberately use a further simplified model to demonstrate the robustness of the scheme. The control design model additionally assumes small angle rotations and uniform charge distributions. Which results in $f^e_{11} = \frac{-1}{\epsilon A}$, $f^e_{22} = \frac{-1}{\epsilon A}$, $T^e_{11} = \frac{l}{2\epsilon A}$ and $T^e_{22} = \frac{-l}{2\epsilon A}$.

The open-loop system (12)–(14) then takes the explicit form

$$\dot{Q}_1 = -\frac{1}{r_1}(V_1 - u_1), \tag{18}$$

$$\dot{Q}_2 = -\frac{1}{r_2}(V_2 - u_2), \tag{19}$$

$$\dot{x} = v, \tag{20}$$

$$\dot{\theta} = \alpha, \tag{21}$$

$$\dot{v} = -2\zeta_x\omega_x v - \omega_x^2(x-d) + \frac{1}{2m}\begin{bmatrix} Q_1 & Q_2 \end{bmatrix} f^e \begin{bmatrix} Q_1 \\ Q_2 \end{bmatrix}, \tag{22}$$

$$\dot{\alpha} = -2\zeta_\theta\omega_\theta\alpha - \omega_\theta^2\theta + \frac{1}{2I}\begin{bmatrix} Q_1 & Q_2 \end{bmatrix} T^e \begin{bmatrix} Q_1 \\ Q_2 \end{bmatrix}. \tag{23}$$

The stabilizing control (16) reduces to

$$u_1 = V_1 - r_1\frac{(Q_1 + \bar{Q}_1)}{2}(vf^e_{11} + \alpha T^e_{11}) - r_1 k(Q_1 - \bar{Q}_1), \tag{24}$$

$$u_2 = V_2 - r_2\frac{(Q_2 + \bar{Q}_2)}{2}(vf^e_{22} + \alpha T^e_{22}) - r_2 k(Q_2 - \bar{Q}_2), \tag{25}$$

where α is the angular velocity and v is the velocity of the center of mass of the movable top electrode. We choose $K = diag(k, k)$ for $k > 0$.

The static and dynamic output feedback controllers for this model are tested in a 3-D, multiphysics, ANSYS simulation. These finite-element simulations include flexibility and full translational and rotational motion of the mirror, fringing of the electrostatic field, geometric nonlinearities, and electrode-to-electrode coupling [53]. It neglects parasitic capacitances, however. The ANSYS model is shown in figure 1. The cantilever beams and movable electrode plate are aluminum. The movable electrode dimensions are 100 μm $\times$ 100 μm $\times$ 2 μm. The

Copyright © 2005 John Wiley & Sons, Ltd.

cantilever thickness is 8 μm and the gap between the cantilever arms and the mirror plate is 12 μm. The zero voltage gap between the movable top electrode and the fixed bottom electrodes is 3.5 μm. The two bottom control electrodes are each 50 μm $\times$ 100 μm.

The controllers are implemented in an ANSYS macro. Figure 2–3 shows the effectiveness of charge feedback control (15) in stabilizing beyond pull-in. All dimensions are in microns, with time in seconds. The dynamic feedback results are shown in Figure 4–5. A comparison of figures (2)–(4) shows the improvement in overshoot and settling time when velocity feedback (24)–(25) is used. Transient response of the system can be further improved by adjusting the gain k. In spite of the extreme simplification of the control model, performance is seen to be very satisfactory. We stress again that the ANSYS simulation does not include any of the simplifying assumptions of the control model, except for the lack of parasitics.

5. Conclusion

We have presented a general geometric formulation for the control of electrostatically-actuated devices, including MEMS and potentially NEMS. A general form of the governing equations is presented, valid for devices whose configuration space may be written as a Lie group, and whose kinetic energy is left invariant. It is shown that a passivity-based control approach may be applied to systems of this form, to stabilize any feasible equilibrium point. Both robust static output feedback, for pure stabilization, and robust dynamic output feedback, for stabilization plus improved transient response, are given. The geometric formulation is specified for a MEMS device of interest, and the results validated using finite-element ANSYS simulations.

The geometric approach provides a very powerful framework in which dynamics may be analyzed, controllers designed, and important properties proved, with the resulting conclusions then applicable to a very broad class of devices. Future work in this area will include adaptive controllers for insensitivity to parameter uncertainty.

A number of important considerations are omitted here, notably the physical implementation of the controllers. For MEMS devices, on-chip analog circuitry may be used to obtain charge and capacitance measurements. The static output feedback strategies are well within current practice. Implementation of the dynamic output feedback controller is a topic of future study, but should not be much more involved than implementing a standard Luenberger observer. For NEMS the topic is entirely open, like many issues in this emerging area.

Acknowledgments

The support of the National Science Foundation under grants ECS0218345 and ECS0220314 is gratefully acknowledged. The authors would also like to thank an anonymous reviewer for extensive remarks that not only greatly improved the present paper, but suggested intriguing directions for future study.

REFERENCES

1. R. Abraham and J. E. Marsden, *Foundations of Mechanics, Second Ed.* Westview, 1978.

Copyright © 2005 John Wiley & Sons, Ltd.

2. N. Aghannan and P. Rouchon, “An Intrinsic Observer for a Class of Lagrangian Systems,” *IEEE Transactions on Automatic Control*, (48) No. 6, pp 936–945, June 2003.
3. R. C. Anderson, B. Kawade, D. H. S. Maithripala, K. Ragulan, J. M. Berg, R. O. Gale, “Integrated charge sensors for feedback control of electrostatic MEMS,” *Proceedings of the SPIE conference on Smart Structures and Materials 2005: Sensors and Smart Structures Technologies for Civil, Mechanical, and Aerospace Systems*, San Diego, 6-10 March 2005.
4. F. Ayela, J. L. Bret, J. Chaussy, T. Fournier and E. Menegaz, “A Two-Axis Micromachined Silicon Actuator with Micrometer Range Electrostatic Actuation and Picometer Sensitive Capacitive Detection,” *Review of Scientific Instruments*, Vol. 71, Number 5, ppg 2211–2218, May 2000.
5. A. M. Bloch, J. Baillieul, P. Crouch and J. E. Marsden, *Nonholonomic Mechanics and Control,* Springer-Verlag, New York 2003.
6. D. M. Bloom, “The Grating Light Valve: Revolutionizing Display Technology, ” *Projection Displays III Symposium, SPIE Proceedings Volume 3013*, February 1997.
7. F. Bullo and A. D. Lewis, *Geometric Control of Mechanical Systems: Modeling, Analysis, and Design for Simple Mechanical Control Systems,* Springer-Verlag, New York 2004.
8. C. I. Byrnes, A. Isidori and J. C. Willems, “Passivity, Feedback Equivalence, and the Global Stabilization of Minimum Phase Nonlinear Systems,” *IEEE Transactions on Automatic Control*, (36) No. 11, ppg 1228 – 1240, Nov 1991.
9. E. K. Chan, R. W. Dutton, “Electrostatic micromechanical actuator with extended range of travel,”, *Journal of Microelectromechanical Systems*, Vol. 9, No. 3, pp. 321–328, 2000.
10. H. C. Larnaudie, F. Rivoirard and B. Jammes, “Analytical Simulation of a 1D Single Crystal Silicon Electrostatic Micromirror,” *Proc. of the Second Int. Conf. on Modelling and Simulation of Microsystems, Semiconductors, Sensors and Actuators, Chicago, CA*, ppg 628–631, April 1999.
11. P. B. Chu, Shi-Sheng Lee, and S. Park, “MEMS: The Path to Large Optical Crossconnects,” *IEEE Communications Magazine*, ppg 80–87, March 2002.
12. S. Chung, and Y. Kim, “Design and Fabrication of a 10 × 10 micro-spatial Light Modulator Array for Phase and Amplitude Modulation ,” *Sensors and Actuators*,Vol 78 pp. 63–70, 1999.
13. J. Comtois, A. Michalicek, W. Cowan, and J. Butler, “Surface-micromachined Polysilicon MOEMS for Adaptive Optics,” *Sensors and Actuators*,Vol 78 pp. 54–62, 1999.
14. D. Elata, O. Bochobza-Degni and Y. Nemirovsky, “Analytical Approach and Numerical alpha-line method for Pull-In Hyper-surface Extraction of Electrostatic Actuators with Multiple Uncoupled Voltage Sources,” *Journal of Microelectromechanical Systems,* Vol. 12, No. 5, pp. 681–691, Oct 2003.
15. A. M. Fennimore, T. D. Yuzvinsky, W.-Q. Han, M. S. Fuhrer, J. Cumings and A. Zetti, “Rotational Actuators Based on CArbon Nanotubes,” *Nature*, Vol.424, July 2003.
16. R. P. Feynman, R. B. Leighton and M. Sands, “The Feynman Lectures on Physics: Electro Magnetic Fields,” *Reading, Mass, Adison-Wesley Pub. Co.*, 1963.
17. J. M. Florence and R. O. Gale, “Coherent optical correlator using a deformable mirror device spatial light modulator in the Fourier plane,” *Applied Optics*, Vol. 27, No. 11, pp. 2091–2093, 1988.
18. L. J. Hornbeck, “From cathode rays to digital micromirrors: A history of electronic projection display technology,” *TI Technical Journal*, July–September, pp. 7–46, 1998
19. A. Isidori, *Nonlinear Control Systems,* 3rd Ed., Springer-Verlag, London 1995.
20. A. G. Kelkar, S. M. Joshi and T. E. Alberts, 1995, “Passivity Based Control of Nonlinear Flexible Multibody Systems”, *IEEE Trans. Automat. Control*, 40 (5), pp. 910–914.
21. G. T. A. Kovacs, *Micromachined Transducers Sourcebook,* McGraw-Hill, New York, 1998.
22. J. M. Kyynarainen, A. S. Oja and H. Seppa, ”Increasing the Dynamic Range of a Micromechanical Moving-Plate Capacitor,” *Journal of Analog Integrated Circuits and Signal Processing*, 29 pp. 61–70, 2001.
23. M. S.-C. Lu and G. K. Fedder, “Position Control of Parallel-Plate Microactuators for Probe-Based Data Storage,” *Journal of Microelectromechanical Systems*, Vol. 13, No. 5, October 2004, pp. 759–769.
24. D. H. S. Maithripala, J. M. Berg and W. P. Dayawansa, “An Intrinsic Observer for a Class of Simple Mechanical Systems on Lie Groups,” *Proceedings of the ACC 2004*, Boston, 2004.
25. D. H. S. Maithripala, J. M. Berg and W. P. Dayawansa, “Nonlinear Dynamic Output Feedback Stabilization of Electrostatically-Actuated MEMS,” *Proc. of the CDC*, Maui, HW, 2003.
26. D. H. S. Maithripala, R. O. Gale, M. W. Holtz, J. M. Berg and W. P. Dayawansa, “Nano-precision control of micromirrors using output feedback,” *Proc. of the CDC*, Maui, HW, 2003.
27. D. H. S. Maithripala, J. M. Berg and W. P. Dayawansa, “Control of an Electrostatic MEMS Using Static and Dynamic Output Feedback,” *ASME Journal of Dynamical Systems Measurement and Control*, to appear.
28. D. H. S. Maithripala, W. P. Dayawansa and J. M. Berg “Intrinsic Observer-Based Stabilization fo Simple Mechanical Systems on Lie Groups,” *SIAM journal on control and optimization*, to appear.
29. D. H. S. Maithripala, J. M. Berg and W. P. Dayawansa, “State and Configuration Feedback for Almost Global Tracking of Simple Mechanical Systems on a General Class of Lie Groups,” *IEEE Transactions on*

Copyright © 2005 John Wiley & Sons, Ltd.

Automatic Control, to appear.
30. J. E. Marsden and T. S. Ratiu, *Introduction to Mechanics and Symmetry, Second Ed.* Springer-Verlag, New York 1999.
31. B. McCarthy, G. G. Adams, N. E. McGruer and D. Potter, ‘ ‘A Dynamic Model, Including Contact Bounce, of an Electrostatically Actuated Microswitch,” *Journal of Microelectromechanical Systems,* Vol. 11, No. 3, pp. 276–283, June 2002.
32. R. E. Meier, “DMD pixel mechanics simulation,” *TI Technical Journal*, Special issue on DLP—DMD Manufacturing and Design Challenges, July–September, 1998, pp. 64–74.
33. R. Nadal-Guardia, A. Dehe, R. Aigner and L. MĊastaner, “Current drive methods to extend the range of travel of electrostatic microactuators beyond the voltage pull-in point,” *Journal of Microelectromechanical Systems,* Vol. 11, No. 3, pp. 255–263, June 2002.
34. M. Napoli, W. Zhang, K. Turner and B. Bamieh, “Characterization of Electrostatically Coupled Microcantilevers,” *Journal of Microelectromechanical Systems,* Vol. 14, No. 2, pp. 295–304, April 2005.
35. Nathanson H. C., Newell W. E., Wickstrom R. A. and Davis J. R., 1967, “The Resonant Gate Transistor”, *IEEE Trans. on Electron Devices,*, **14** (3), pp. 117–133.
36. Y. Nemirovsky and O. Bochobza-Degni, “A Methodology for the Pull-In Parameters of Electrostatic Actuators,” *Journal of Microelectromechanical Systems,* Vol. 10, No. 4, pp. 601–615, Dec 2001.
37. R. Ortega, A. J. van der Schaft, I. Mareels and B. Maschke, 2001, “Putting Energy Back in Control,” *IEEE Control Systems Magazine*, April, pp 18-33.
38. R. Ortega and Romeo Ortega and Eloisa Garcia-Canseco, 2004, “Interconnection and Damping Assignment Passivity Based Control: A Survey,” *To appear in the European Journal of Control*, April, pp 18-33.
39. J. A. Pelesko and Triolo A. A., 2001, “Nonlocal Problems in MEMS Device Control,” *J. of Enginering Mathematics* **41** (4), 345 – 366.
40. J. A. Pelesko, “Mathematical Modeling of Electrostatic MEMS with Tailored Dielectric Properties,” *SIAM J. Appl. Math.* vol. 62, 888-908, 2002.
41. J. A. Pelesko and D. H. Bernstien, *Modeling MEMS and NEMS* Chapman and Hall, CRC Press, 2002.
42. J. A. Pelesko and T. A. Driscoll, 2004, “Approximatons in Canonical Electrostatic MEMS Models,” *Internal Report: http://dspace.udel.edu:8080/dspace/handle/19716/208* Sep. 2004.
43. H. S. Sane, N. Yazdi and C. H. Mastrangelo, “Application of Sliding Mode Control to Electrostatically Actuated Two-Axis Gimbaled Micromirrors,” *Proc. of the American Control Conference, Denver, CO*, June, pp. 3726–3721, 2003.
44. J. I. Seeger and S. B. Crary, “Stabilization of Electrostatically Actuated Mechanical Devices,” *Proc. of the Ninth Int. Conf. on Solid-State Sensors and Actuators (Transducers ’97)*, Chicago, IL, June 16-19, pp. 1133–1136, 1997.
45. J. I. Seeger and B. E. Boser, “Dynamics and Control of Parallel-Plate Actuators Beyond the Electrostatic Instability,” *Proc. of the Tenth Int. Conf. on Solid-State Sensors and Actuators (Transducers ’99)*, Sendai, Japan, June 7-9, pp. 474–477, 1999.
46. J. I. Seeger and B. E. Boser, “Charge Control of Parallel-Plate, Electrostatic Actuators and the Tip-In Instability,” *Journal of Microelectromechanical Systems,* Vol. 12, No. 5, pp. 656–671, October 2003.
47. R. Sepulchre, M. Jankovic and P. Kokotovic, *Constructive Nonlinear Control,* Springer-Verlag, London 1997.
48. Stephen D. Senturia, *Microsystem Design*, Kluwer Academic Publishers, Norwell, MA 2001.
49. H. Toshiyoshi, M. Mita, H. Fujita, “A MEMS Piggyback Actuator for Hard-Disk Drives,” *J. of Microelectromechanical Systems*, Vol. 11, No. 6, 2002, pp. 648–654.
50. Y. Yee, H.-J. Nam, S.-H. Le, J. U. Bu, and J.-W. Lee, “PZT Actuated Micromirror for Fine-Tracking Mechanism of High-Density Optical Data Storage” *Sensors and Actuators* vol. 2864, 1-8 (2000).
51. G. Zhu, J. Levine, and L. Praly, “On the Differential Flatness and Control of Electrostatically Actuated MEMS,” *Proceedings of the ACC*, Portland, Oregon, 2005.
52. “Analyzing Hazards from a Distance”, *Sandia Technology. a Quarterly Research and Development Journal* vol.4 (3), pp. 11–12, Fall 2002.
53. “ANSYS Release 8.1 Documentation”, *ANSYS, Inc.*, Canonsburg, PA, 2004.

Copyright © 2005 John Wiley & Sons, Ltd.

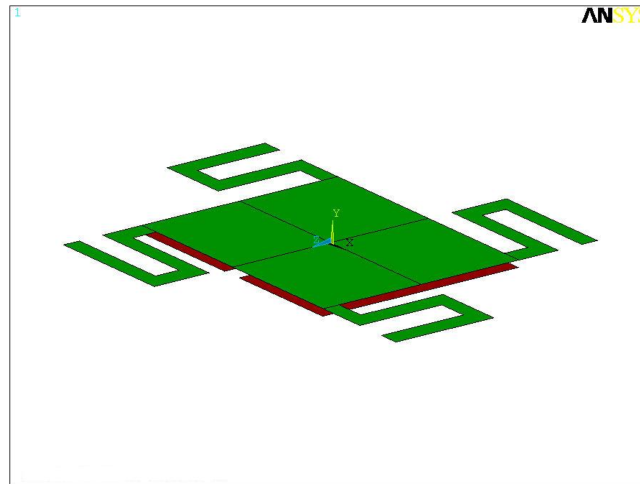

Figure 1. ANSYS model of electrostatic MEMS. Movable mirror suspended on four flexures over two fixed control electrodes.

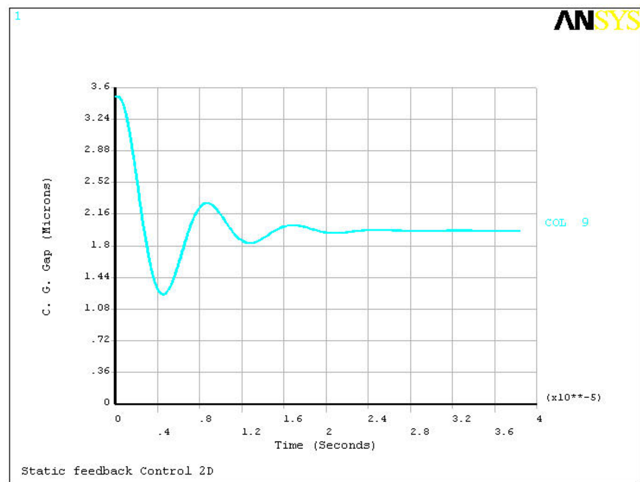

Figure 2. The displacement of the center of mass in the vertical direction for the charge feedback control (15).

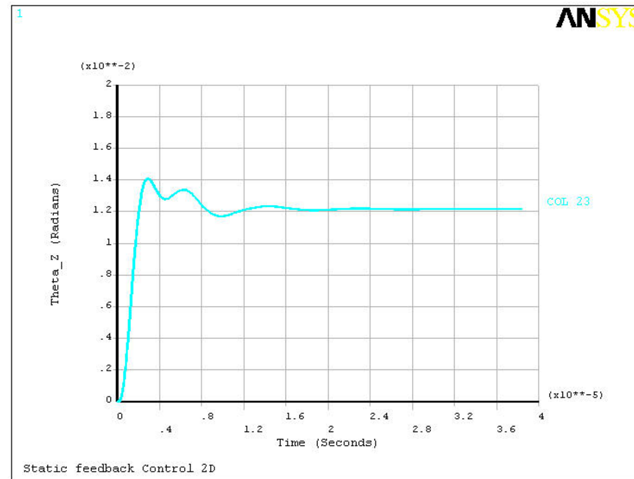

Figure 3. The angular displacement about the out-of-plane direction for the charge feedback control (15).

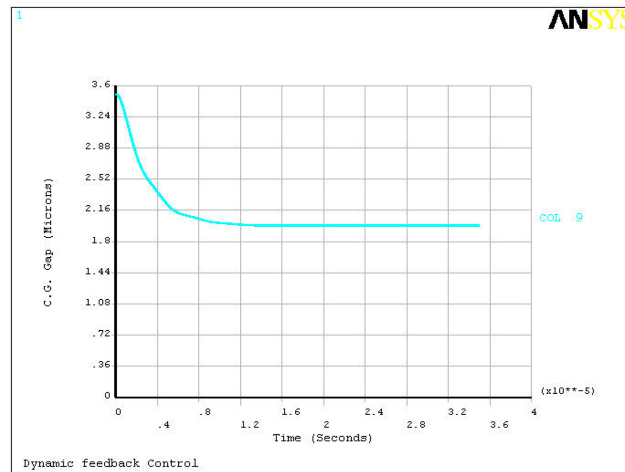

Figure 4. The displacement of the center of mass in the vertical direction for the velocity feedback control (24)–(25).

Copyright © 2005 John Wiley & Sons, Ltd.

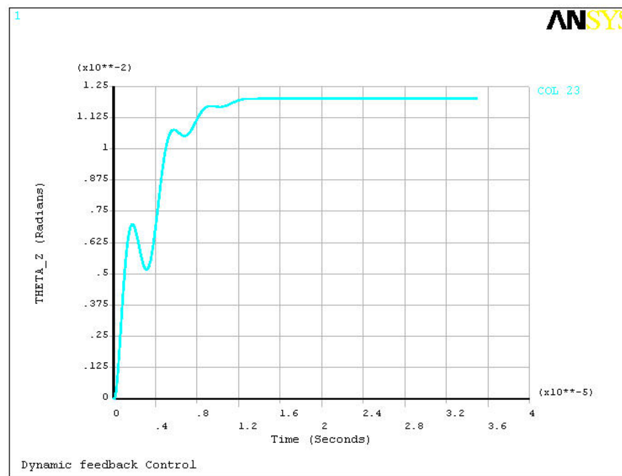

Figure 5. The angular displacement about the out-of-plane direction for the velocity feedback control (24)–(25).

Copyright © 2005 John Wiley & Sons, Ltd.

Prepared using rncauth.cls